Lithuanian Journal of Physics
Vol. **65**, No. 4, pp. 258–265 (2025)
ISSN 1648-8504 eISSN 2424-3647
DOI: https://doi.org/10.3952/physics.2025.65.4.8

FABRICATION AND MAGNETORESISTIVE PROPERTIES OF MAGNETRON-SPUTTERED CoFe/Cu SPIN VALVES WITH ANTIFERROMAGNETIC IrMn PINNING

V. Vertelis [a, b], D. Antonovič [a], S. Keršulis [a], A. Maneikis [a], and N. Žurauskienė [a, b]

[a] *Department of Functional Materials and Electronics, Center for Physical Sciences and Technology, Saulėtekio 3, 10257 Vilnius, Lithuania*

[b] *Faculty of Electronics, Vilnius Gediminas Technical University, Saulėtekio 11, 10223 Vilnius, Lithuania*

Email: vilius.vertelis@ftmc.lt

Received 4 December 2025; accepted 5 December 2025

Nanolayered ferromagnetic/non-magnetic structures exhibit the giant magnetoresistance (GMR) effect and are used in a variety of applications. Spin valves are one class of devices that fall into the GMR category. In this work, the fabrication and characterization results of magnetron sputtered Ta/IrMn/CoFe/Cu/CoFe/Ta spin valve structures are presented. Two groups of samples were produced where the thickness of the Cu spacer layer or the CoFe pinned layer were varied in search of the highest magnetoresistance value. The maximum value of 4.8% magnetoresistance was obtained for a sample with the composition of Ta(5 nm) / IrMn(15 nm) / CoFe(2 nm) / Cu(2 nm) / CoFe(5 nm) / Ta(5 nm) when the sample was shaped into a meandering channel with 2 μm width. The achieved results are promising and will be used to further develop spin valve technology for various applications.

Keywords: spin valve, magnetoresistance, spintronics

1. Introduction

Spintronics is a field of solid-state physics aimed at utilizing electron spin, a fundamental property of the electron, in solid state devices, and focuses on spin polarization, injection, transfer and manipulation. Spin valves are spintronic devices that exhibit giant magnetoresistance (GMR), caused by spin-dependant scattering in ferromagnetic materials. The GMR effect was simultaneously discovered by both Fert's [1] and Grünberg's [2] research teams in Fe and Cr multilayered nanostructures during the 1980's. They were awarded the Nobel Prize for this work. Those structures were composed of nm thick ferromagnetic (FM) Fe layers separated by nm thick non-magnetic (NM) Cr layers of precise thickness to establish antiparallel magnetization alignments in the Fe layers due to the Ruderman–Kittel–Kasuya–Yosida (RKKY) interaction. An external magnetic field aligns the magnetizations of the ferromagnetic layers, leading to a reduction in the resistivity across the entire structure. Spin valve structures, on the other hand, are constructed from at least two ferromagnetic layers separated by a non-magnetic spacer that can either be conductive or insulating, the latter being called a tunnelling magnetic junction (TMJ) [3]. In these structures, magnetoresistance is achieved by ensuring that the magnetization curves are different between the FM layers. One layer is usually stabilized or 'pinned', making it harder to change its magnetization. Traditional spin valves achieve this by using the same FM materials and pinning is done by growing one of the FM layers on an antiferromagnetic (AF) material, causing the magnetization curve to shift due to exchange bias. The layer can also be pinned by forming synthetic antiferromagnets (SAF) where the exchange bias can be tuned [4–6]. This is done by forming another FM/NM/FM trilayer with a carefully controlled spacer thickness. Magnetization separation can also be achieved by combining different soft (free layer) and hard (reference or pinned layer) FM materials [7] or having different FM layer thicknesses [8]. Such devices are called pseudo-spin valves (PSV). With the discovery of 2D ferromagnetism in 2017

[9], a new field on van der Waals (vdW) spin valves emerged [10–12] with an added tunability with gating [13].

GMR-based devices have achieved a wide array of applications due to their low power usage and cost-efficiency. One of the most prominent fields is data storage, where spin valves and TMJs are used as read heads in hard disk drives (HDDs) [14] and in magnetic random-access memory (MRAM) [15], which is non-volatile, durable, and consumes little power [16]. Similarly, spin logic devices that employ GMR are also actively investigated [17]. Industrial applications include ammeters [18], position sensors [19], and non-destructive testing [20]. Advances have been made in GMR-based biomedical applications including point-of-care disease diagnosis [21–23], genotyping [24], food and drug regulation [25], brain and cardiac mapping [26]. Another area of interest is position sensing with GMR sensors being fitted in traffic speed monitors and car positioning systems [27].

Although spin valve structures and IrMn pinning are well-established, this work focuses on developing a reproducible fabrication and characterization workflow tailored for research environments, enabling a precise control of layer thickness and geometry. By achieving magnetoresistance values up to 4.8% in meander-shaped microstructures, we demonstrate performance comparable to state-of-the-art devices while introducing geometries optimized for sensor integration. These results provide a critical step toward adapting conventional spin valve technology for emerging applications such as biosensing and van der Waals heterostructures, where miniaturization and a high sensitivity are essential.

2. Methods

Heterostructures were grown on a rotating (10 rpm) Si/SiO_2 (with 300 nm thick SiO_2 layer, roughness average $R_a < 0.5$ nm) substrate using a magnetron sputtering system (TFSP – 840, *Vacuum Systems Technology*, Israel). Layers were deposited at room temperature in the Ar atmosphere (4 mTorr). Ta(5 nm) / IrMn(15 nm) / CoFe(x) / Cu(y) / CoFe(z) / Ta(5 nm) structures were grown in the provided sequence. The structure was chosen as a benchmark because of its simplicity and multiple examples found in the literature. Ta, $Ir_{0.2}Mn_{0.8}$ and $Co_{0.9}Fe_{0.1}$ layers were DC sputtered at 0.7, 0.8 and 1.7 nm/min, respectively, while Cu was RF sputtered at 1.25 nm/min. Ta layers were used both to form a smooth base layer for the magnetic heterostructure and to passivate the devices. CoFe layers were used for their ferromagnetic properties. IrMn is an antiferromagnet and was used for pinning one of the CoFe layers, shifting its magnetization curve thus making it different from the free CoFe layer's magnetization. Cu was used as a non-magnetic conductive separator between the ferromagnetic layers.

After deposition, the heterostructures were annealed at 200°C in a 100 mT external magnetic field and Ar atmosphere for 30 min, after which the samples were allowed to cool to room temperature in the Ar atmosphere in the same magnetic field which took about an hour. That was done to set the preferred magnetization direction in the structure.

After the annealing procedures, the substrates were scribed and cleaved to form ~1 × 2 mm samples. The samples were then transferred onto a sample holder and secured using cyanoacrylate. Wires were bonded using conductive silver paste.

Magnetoresistance measurements were conducted in the current-in-plane (CIP) mode, where the current density vector is perpendicular to the normal vector of the structure (see Fig. 1). The two-terminal method was used. The magnetic flux density was ramped up from zero to 90 mT, then brought down to zero, after which the polarity was changed and the process repeated. This cycling was done several times in order to establish a stable magnetoresistance curve.

3. Results and discussion

A series of heterostructures was grown, varying the thicknesses of the Cu and pinned CoFe layers. Cu thickness is a key parameter determining the magnetic coupling between the FM layers via RKKY interaction [28]. The list of thicknesses is given in Table 1. Samples in Group I (G98, G101, G102 and G103) were used for tuning the thickness of the non-magnetic (NM) Cu spacer layer that was sandwiched between two layers of CoFe. Parameters of the non-Cu layers were not modified at this stage. Samples in Group 2 (G105, G139, G141 and G144) had a stable Cu layer thickness of

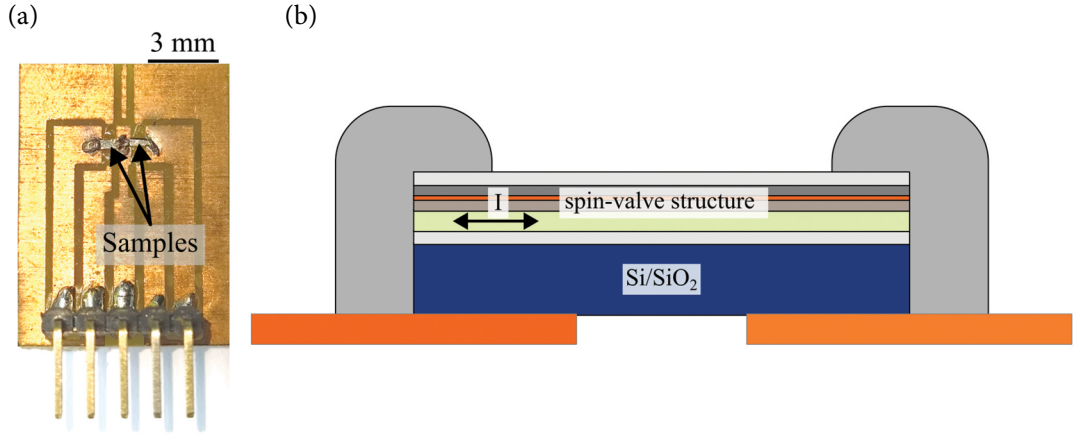

Fig. 1. Formed samples secured to a holder (a). Illustration of a cross-sectional view of the sample with electrical contacts and current direction indicated (b).

Table 1. List of grown heterostructures Ta(5 nm) / IrMn(15 nm) / CoFe(x) / Cu(y)/CoFe(5 nm) / Ta(5 nm).

		x, nm	y, nm
Group I	G98	5	2.5
	G101	5	2
	G102	5	3.3
	G103	5	3
Group II	G105	2	2
	G139	4	2
	G141	4	2

2 nm, but the thickness of the pinned CoFe layer varied from 2 to 4 nm. Sample G141 had the same layer structure as G139 but was formed into meander-like strips with a 2 μm width (see Fig. 2) to test and enable geometries required for future applications, such as nanoparticle detection. This was done using standard photolithography and Ar ion milling. G144 had its layer structure inverted with respect to G139: Ta(5 nm) / CoFe(5 nm) / Cu(2 nm) / CoFe(4 nm) / IrMn(15 nm) / Ta(5 nm).

The quality of the deposited structures and their layer composition was analyzed using transmission electron microscopy (TEM) and energy-dispersive X-ray spectroscopy (EDX). The results are presented in Fig. 3. Layers of the spin valve structure were smooth and continuous. The transitions between the layers were sharp, intermixing between the layers was not observed or was smaller than the spatial resolution of the device. The layer obtained thicknesses were within 0.5 nm to their target values.

Figure 4 represents the magnetoresistance measurement results for the first group of samples at two different magnetic field orientations: parallel and perpendicular to the magnetic field

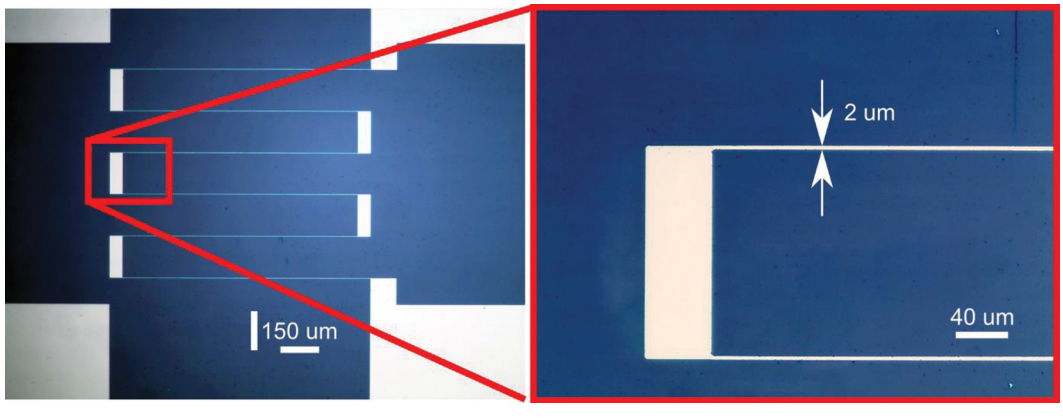

Fig. 2. Micrograph of the top view of sample G141, which was formed into a meandering 2 μm wide strip.

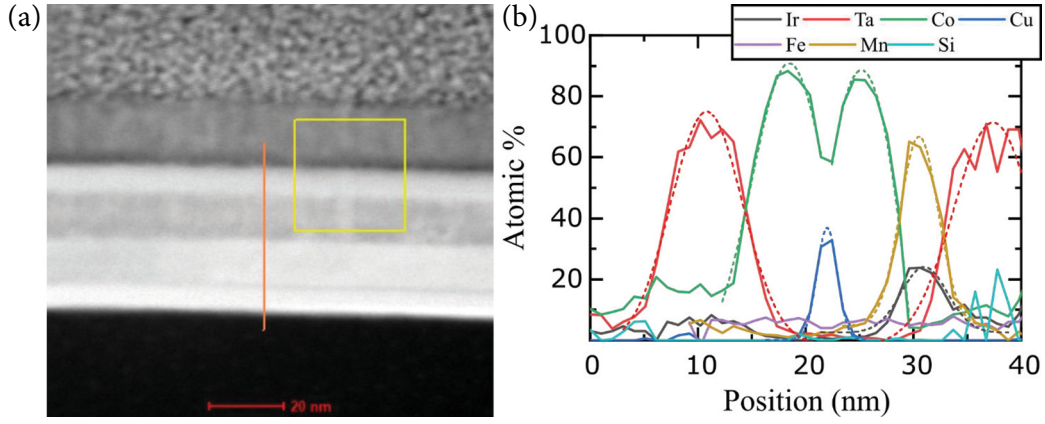

Fig. 3. TEM image of the cross-section of the G101 heterostructure (a), EDX elemental percentages along the trace line (orange line in (a)), (b).

direction during annealing. It must be addressed that the absolute magnetoresistance values could have been influenced by contact resistance as the two-terminal method was used to measure sample resistances. Despite that, curve shapes convey information about the structure's magnetic properties and spin dependent scattering. Magnetoresistance MR is defined as

$$MR(B) = \frac{R(B) - R_{\uparrow\uparrow}}{R_{\uparrow\uparrow}} \cdot 100\%, \quad (1)$$

where $R(B)$ is the sample's resistance exposed to the magnetic flux density B, and $R_{\uparrow\uparrow}$ is the resistance in the parallel magnetization state (lowest resistance). As can be seen, the MR curves for Group I samples all had a similar shape. A peak magnetoresistance of 1.3% was observed in sample G102 at 2.2 mT. A single magnetoresistance peak was observed during a full magnetic flux density sweep (from +90 mT to −90 mT and vice versa) at around ±2.5 mT. The sign was determined by the direction of the magnetic field sweep. The resistance of the structure depends on the angle θ between the magnetization vectors of the ferromagnetic layers [29] and is defined as

$$R(\theta) = R_{\uparrow\uparrow} + (R_{\uparrow\downarrow} - R_{\uparrow\uparrow})\frac{1 - \cos\theta}{2}. \quad (2)$$

Such a magnetoresistance curve shape indicated that the antiferromagnetic pinning was not established and that the angle between the magnetization directions was only determined by the intrinsic magnetization curve of each layer. The devices behaved as PSVs. Since the pinned CoFe layer thicknesses were the same, the mag-

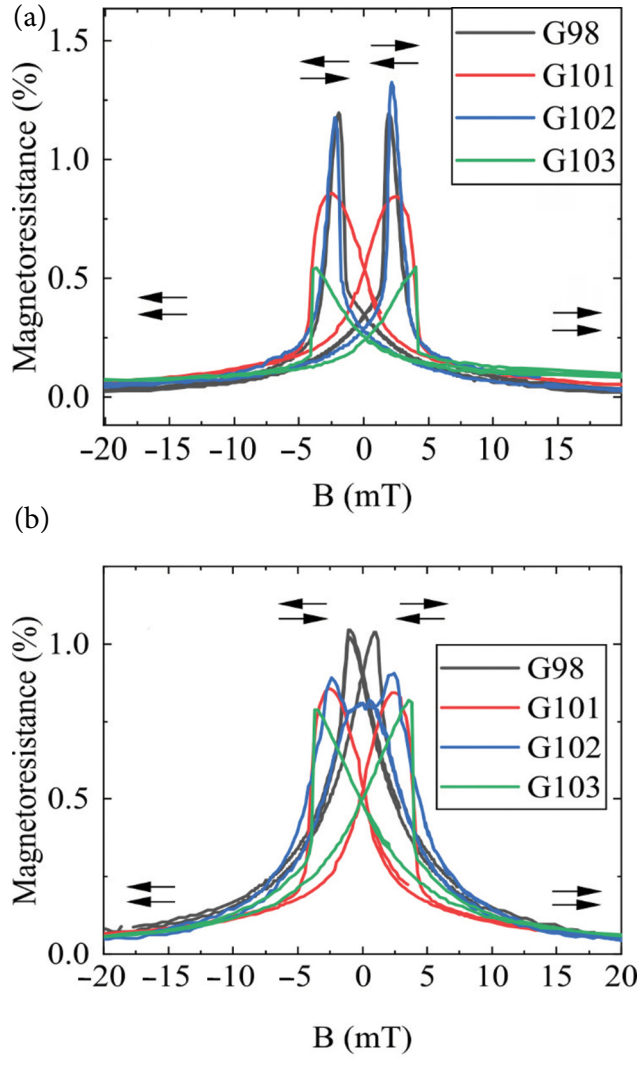

Fig. 4. Magnetoresistance curves of the spin valves exposed to magnetic field in line with the direction of the applied magnetic field during annealing (a). Magnetoresistance curves of the spin valves exposed to a magnetic field perpendicular to the direction of the applied magnetic field during annealing (b).

netization curves could only differ slightly and only small angles between the magnetizations could be achieved resulting in sub-optimal magnetoresistance. Poor antiferromagnetic pinning could also have been caused by the surface oxidation of the IrMn target and insufficient cleaning before deposition.

The magnetoresistance curves differed depending on the field direction. Larger peak-magnetoresistance was observed when the external field was in the same direction as the field during annealing. Peak magnetoresistance vs copper spacer thickness is given in Fig. 5. An oscillatory behaviour with a period of ~1 nm can be seen that is in accordance with the RKKY model. In the perpendicular field mode, the magnetoresistance curves were symmetric regardless of the sample; however, the peak magnetoresistance was decreased due to the maximum angle between the layer magnetizations being 90° in this configuration.

Group II samples had higher magnetoresistances and antisymmetric magnetoresistance curves. The full extent of the measurements is presented in Fig. 6. A peak magnetoresistance was obtained with G141 and was equal to 4.8%, which is comparable to values reported in the literature for CoFe spin valves [30–32]. This increased magnetoresistance can be attributed to the reduced number of defects in thin strips and a shape-induced demagnetization field, which helps align the magnetizations of the layers along the length

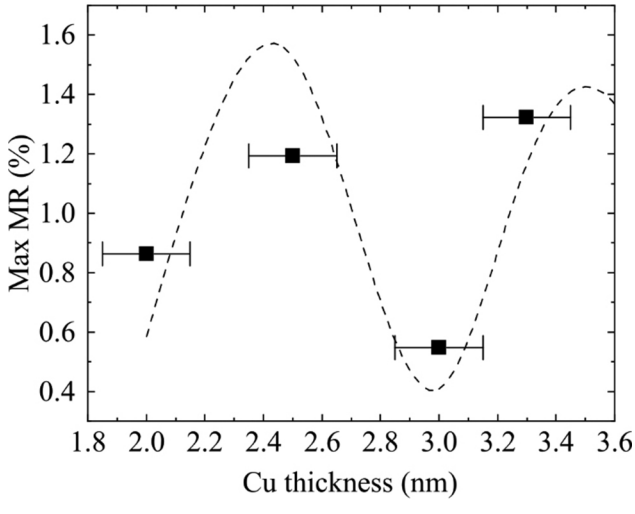

Fig. 5. Peak magnetoresistance dependence on the Cu separator layer thickness. Dotted line is a guide to the eyes.

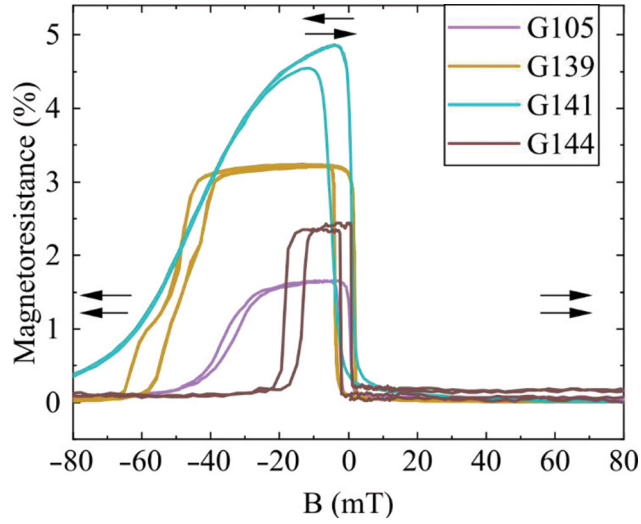

Fig. 6. Magnetoresistance curves of Group II samples. Arrows indicate relative magnetization directions.

of the strip. The inverted structure of sample G144 resulted in a reduced magnetoresistance when compared to G139.

Group II samples showed antisymmetric magnetoresistance curves with a hysteresis centred at 0 mT. Such magnetoresistance curves indicate that the CoFe layers that were grown on the antiferromagnetic IrMn were magnetically pinned and had a preferred direction of magnetization while the second CoFe layer did not. For this group, IrMn targets were cleaned for longer time before the deposition process. That, in combination with a different thickness of the pinned CoFe layers, resulted in substantially differing magnetization curves of the CoFe layers and led to an effective structure where the magnetization directions could be different, leading to an increased magnetoresistance.

4. Conclusions

CoFe/Cu-based antiferromagnetically biased spin valves were successfully produced and analyzed. The magnetron sputtering process, combined with controlled annealing and sample preparation, enabled the growth of multilayered structures with sub-nanometre accuracy and sharp interfacial transitions. TEM and EDX analyses confirmed the structural integrity and compositional fidelity of the layers, validating the effectiveness of the deposition parameters and post-processing steps.

Magnetoresistance measurements, conducted using a CIP two-terminal setup, provided clear

insights into the magnetic behaviour of the samples. Despite the limitations posed by contact resistance, the observed MR curves were consistent and informative, revealing spin-dependent scattering, magnetic pinning, and RKKY oscillations. The enhanced performance in Group II highlights the importance of layer thickness optimization, target purity, and structural geometry in achieving the desired magnetic properties with magnetoresistance values close to reported values. A peak magnetoresistance of 4.8% was achieved in the CIP configuration in a sample shaped into a meandering 2 μm channel. These results lay a solid foundation for future investigations into spintronic devices, including advanced sensor architectures, 2D ferromagnetic material incorporation, memory elements, and biomedical applications.

References

[1] M.N. Baibich, J.M. Broto, A. Fert, F. Nguyen Van Dau, F. Petroff, P. Eitenne, G. Creuzet, A. Friederich, and J. Chazelas, Giant magnetoresistance of (001)Fe/(001)Cr magnetic superlattices, Phys. Rev. Lett. **61**(21), 2472 (1988), https://doi.org/10.1103/PhysRevLett.61.2472

[2] G. Binasch, P. Grünberg, F. Saurenbach, and W. Zinn, Enhanced magnetoresistance in layered magnetic structures with antiferromagnetic interlayer exchange, Phys. Rev. B **39**(7), 4828 (1989), https://doi.org/10.1103/PhysRevB.39.4828

[3] S. Yuasa and D.D. Djayaprawira, Giant tunnel magnetoresistance in magnetic tunnel junctions with a crystalline MgO(001) barrier, J. Phys. D **40**(21), R337 (2007), https://doi.org/10.1088/0022-3727/40/21/R01

[4] R.A. Duine, K.J. Lee, S.S.P. Parkin, and M.D. Stiles, Synthetic antiferromagnetic spintronics, Nat. Phys. **14**(3), 217–219 (2018), https://doi.org/10.1038/s41567-018-0050-y

[5] Y. Han, W. Su, Z. Liu, L. Wang, Z. Hu, Z. Wang, and M. Liu, Engineered spin configuration in spin valve with customized synthetic antiferromagnetic coupling and perpendicular magnetic anisotropy, IEEE Trans. Magn. **61**(10) (2025), https://doi.org/10.1109/tmag.2025.3598105

[6] W.X. Xia, K. Inoue, S. Saito, and M. Takahashi, Effect of Rh spacer on synthetic-antiferromagnetic coupling in FeCoB/Rh/FeCoB films, J. Phys. Conf. Ser., **266**(1), 012064 (2011), https://doi.org/10.1088/1742-6596/266/1/012064

[7] J. Dubowik, F. Stobiecki, B. Szymański, I. Gościańska, K. Röll, and Y.P. Lee, Pseudo spin-valve structures with NiO/Co as a hard magnetic layer, Phys. Status Solidi B **241**(7), 1613–1616 (2004), https://doi.org/10.1002/pssb.200304642

[8] N. Thiyagarajah, H.W. Joo, and S. Bae, High magnetic and thermal stability of nanopatterned [Co/Pd] based pseudo spin-valves with perpendicular anisotropy for 1 Gb magnetic random access memory applications, Appl. Phys. Lett. **95**(23), 32 (2009), https://doi.org/10.1063/1.3273374

[9] C. Gong, L. Li, Z. Li, H. Ji, A. Stern, Y. Xia, T. Cao, W. Bao, C. Wang, Y. Wang, Z.Q. Qiu, R.J. Cava, S.G. Louie, J. Xia, and X. Zhang, Discovery of intrinsic ferromagnetism in two-dimensional van der Waals crystals, Nature **546**(7657), 265–269 (2017), https://doi.org/10.1038/nature22060

[10] B. Zhao, R. Ngaloy, S. Ghosh, S. Ershadrad, R. Gupta, K. Ali, A. Md. Hoque, B. Karpiak, D. Khokhriakov, C. Polley, B. Thiagarajan, A. Kaloukhov, P. Svedlindh, B. Sanyal, and S.P. Dash, A room-temperature spin-valve with van der Waals ferromagnet Fe_5GeTe_2/graphene heterostructure, Adv. Mater. **35**(16), 2209113 (2023), https://doi.org/10.1002/adma.202209113

[11] Z. Gao, J. Chen, Z. Zhang, Z. Liu, Y. Zhang, L. Xu, J. Wu, and F. Luo, Large and tunable magnetoresistance in $Cr_{1-x}Te/Al_2O_3/Cr_{1-x}Te$ vertical spin valve device, Adv. Electron. Mater. **9**(1), 2200823 (2023), https://doi.org/10.1002/aelm.202200823

[12] Z. Wang, D. Sapkota, T. Taniguchi, K. Watanabe, D. Mandrus, and A.F. Morpurgo, Tunneling spin valves based on Fe_3GeTe_2/hBN/Fe_3GeTe_2 van der Waals heterostructures, Nano Lett. **18**(7), 4303–4308 (2018), https://doi.org/10.1021/acs.nanolett.8B01278

[13] L. Zhou, J. Huang, M. Tang, C. Qiu, F. Qin, C. Zhang, Z. Li, D. Wu, and H. Yuan, Gate-tunable spin valve effect in Fe_3GeTe_2-based van der Waals heterostructures, InfoMat **5**(3), e12371 (2023), https://doi.org/10.1002/inf2.12371

[14] E.E. Fullerton and J.R. Childress, Spintronics, magnetoresistive heads, and the emergence of the digital world, Proc. IEEE **104**(10), 1787–1795 (2016), https://doi.org/10.1109/jproc.2016.2567778

[15] S. Yang and J. Zhang, Current progress of magnetoresistance sensors, Chemosensors **9**(8), 211 (2021), https://doi.org/10.3390/chemosensors9080211

[16] R. Bishnoi, M. Ebrahimi, F. Oboril, and M.B. Tahoori, Architectural aspects in design and analysis of SOT-based memories, in: Proceedings of the Asia and South Pacific Design Automation Conference ASP-DAC (IEEE, 2014) pp. 700–707, https://doi.org/10.1109/aspdac.2014.6742972

[17] B.B. Vermeulen, B. Sorée, S. Couet, K. Temst, and V.D. Nguyen, Progress in spin logic devices based on domain-wall motion, Micromachines **15**(6), 696 (2024), https://doi.org/10.3390/mi15060696

[18] U.P. Borole, H.C. Barshilia, C.M. Ananda, and P. Chowdhury, Design, Development, and performance evaluation of GMR-based current sensor for industrial and aerospace applications, IEEE Sens. J. **23**(12), 12687–12694 (2023), https://doi.org/10.1109/jsen.2023.3268679

[19] G. Rieger, K. Ludwig, J. Hauch, and W. Clemens, GMR sensors for contactless position detection, Sens. Actuators A **91**(1–2), 7–11 (2001), https://doi.org/10.1016/s0924-4247(01)00480-0

[20] M. Pelkner, R. Stegemann, N. Sonntag, R. Pohl, and M. Kreutzbruck, Benefits of GMR sensors for high spatial resolution NDT applications, AIP Conf. Proc. **1949**(1), 040001 (2018), https://doi.org/10.1063/1.5031535

[21] A. Chicharo, F. Cardoso, S. Cardoso, and P.P. Freitas, Dynamical detection of magnetic nanoparticles in paper microfluidics with spin valve sensors for point-of-care applications, IEEE Trans. Magn. **50**(11) (2014), https://doi.org/10.1109/tmag.2014.2325813

[22] G. Li, S. Sun, R.J. Wilson, R.L. White, N. Pourmand, and S.X. Wang, Spin valve sensors for ultrasensitive detection of superparamagnetic nanoparticles for biological applications, Sens. Actuators A **126**(1), 98–106 (2006), https://doi.org/10.1016/j.sna.2005.10.001

[23] W. Qiu, L. Chang, Y.-C. Liang, J. Litvinov, J. Guo, Y.-T. Chen, B. Vu, K. Kourentzi, S. Xu, T. Randall Lee, Y. Zu, R.C. Willson, and D. Litvinov, Spin-valve based magnetoresistive nanoparticle detector for applications in biosensing, Sens. Actuators A **265**, 174–180 (2017), https://doi.org/10.1016/j.sna.2017.08.018

[24] X. Zhi, M. Deng, H. Yang, G. Gao, K. Wang, H. Fu, Y. Zhang, D. Chen, and D. Cuiet, A novel HBV genotypes detecting system combined with microfluidic chip, loop-mediated isothermal amplification and GMR sensors, Biosens. Bioelectron., **54**, 372–377 (2014), https://doi.org/10.1016/j.bios.2013.11.025

[25] S. Liang, P. Sutham, K. Wu, K. Mallikarjunan, and J.-P. Wang, Giant magnetoresistance biosensors for food safety applications, Sensors **22**(15), 5663 (2022), https://doi.org/10.3390/s22155663

[26] K. Wu, D. Tonini, S. Liang, R. Saha, V.K. Chugh, and J.P. Wang, Giant magnetoresistance biosensors in biomedical applications, ACS Appl. Mater. Interfaces **14**(8), 9945–9969 (2022), https://doi.org/10.1021/acsami.1C20141

[27] K. Wu, D. Su, R. Saha, and J.P. Wang, Giant magnetoresistance (GMR) materials and devices for biomedical and industrial applications, in: Spintronics: Materials, Devices, and Applications (John Wiley & Sons Ltd, 2022) pp. 3–49, https://doi.org/10.1002/9781119698968.ch2

[28] R. Mansell, D.C.M.C. Petit, A. Fernández-Pacheco, R. Lavrijsen, J.H. Lee, and R.P. Cowburn, Magnetic properties and interlayer coupling of epitaxial Co/Cu films on Si, J. Appl. Phys. **116**(6), 63906 (2014), https://doi.org/10.1063/1.4893306

[29] B. Dieny, Giant magnetoresistance in spin-valve multilayers, J. Magn. Magn. Mater. **136**(3), 335–359 (1994), https://doi.org/10.1016/0304-8853(94)00356-4

[30] N.C. Thuan, N. Van Dai, D.N.H. Nam, N.X. Phuc, and L. Van Hong, CIP spin torque effect in the spin valve pinned with an oxide antiferromagnetic layer, J. Phys. Conf. Ser. **187**(1), 012038 (2009), https://doi.org/10.1088/1742-6596/187/1/012038

[31] A.B. Rinkevich, E.A. Kuznetsov, D.V. Perov, M.A. Milyaev, L.I. Naumova, and M.V. Makarova, CoFe/Cu/CoFe/FeMn spin valves and CoFe/Cu/

CoFe three-layer nanostructures at microwave frequencies, Tech. Phys. **69**(4), 1016–1024 (2024), https://doi.org/10.1134/s1063784224030332

[32] P.P. Freitas, R. Ferreira, S. Cardoso, and F. Cardoso, Magnetoresistive sensors, J. Phys. **19**(16), 165221 (2007), https://doi.org/10.1088/0953-8984/19/16/165221

CoFe/Cu SUKINIŲ SKLENDŽIŲ SU PRIRIŠANČIU ANTIFEROMAGNETINIU IrMn SLUOKSNIU GAMYBA MAGNETRONINIO DULKINIMO BŪDU IR MAGNETOVARŽOS TYRIMAS

V. Vertelis [a, b], D. Antonovič [a], S. Keršulis [a], A. Maneikis [a], N. Žurauskienė [a, b]

[a] *Fizinių ir technologijos mokslų centro Funkcinių medžiagų ir elektronikos skyrius, Vilnius, Lietuva*

[b] *Vilniaus Gedimino technikos universiteto Elektronikos fakultetas, Vilnius, Lietuva*

Santrauka

Spintronika – tai kietojo kūno fizikos sritis, nagrinėjanti elektronų sukinio panaudojimą įrenginiuose, daugiausia dėmesio skiriant sukinio poliarizacijai, injekcijai ir manipuliavimui. Dariniai iš feromagnetinių / neferomagnetinių medžiagų nanosluoksnių pasižymi gigantiškos magnetovaržos (GMR) efektu ir yra plačiai naudojami įvairiose srityse. GMR efektas atsiranda dėl nuo sukinio priklausiančios elektronų sklaidos feromagnetinėse medžiagose ir pasireiškia elektrinės varžos pokyčiu keičiantis kampui tarp feromagnetinių sluoksnių įmagnetėjimų. Viena iš tokių įrenginių klasių yra sukinių sklendės (angl. *spin valves*). Šiame darbe pristatomi magnetroninio dulkinimo būdu pagamintų Ta/IrMn/CoFe/Cu/CoFe/Ta sukinių sklendžių darinių gamybos ir charakterizavimo rezultatai. Buvo pagamintos dvi bandinių grupės, kuriose buvo keičiami Cu atskiriamojo sluoksnio arba CoFe pririštojo sluoksnio storiai, siekiant gauti didžiausią magnetovaržos vertę. Didžiausia 4,8 % magnetovarža buvo pasiekta su 2 μm pločio meandro formos bandiniu, kurio sandara yra Ta(5 nm) / IrMn(15 nm) / CoFe(2 nm) / Cu(2 nm) / CoFe(5 nm) / Ta(5 nm). Gauti rezultatai yra perspektyvūs ir bus naudojami tolesniam sukinių sklendžių technologijos vystymui bei taikymui įvairioms reikmėms.